Chemical Science

ROYAL SOCIETY OF CHEMISTRY

EDGE ARTICLE

View Article Online
View Journal | View Issue

Cite this: *Chem. Sci.*, 2023, **14**, 3018

All publication charges for this article have been paid for by the Royal Society of Chemistry

Received 15th November 2022
Accepted 7th February 2023

DOI: 10.1039/d2sc06292e

rsc.li/chemical-science

Photochemical formation and reversible base-induced cleavage of a phosphagallene†

T. Taeufer, [a] F. Dankert, [a] D. Michalik,[ab] J. Pospech, *[a] J. Bresien *[b] and C. Hering-Junghans *[a]

The reactivity of Cp*Ga (Cp* = C_5Me_5) towards phosphanylidenephosphoranes of the type ^{Ar}TerP(PMe_3) (^{Ar}Ter = ^{Dip}Ter 2,6-(2,6-i$Pr_2C_6H_3$)$_2C_6H_3$), ^{Tip}Ter 2,6-(2,4,6-i$Pr_3C_6H_2$)$_2C_6H_3$ was investigated. While no thermal reaction was observed (in line with DFT results), irradiation at 405 nm at low temperatures resulted in the formation of phosphagallenes ^{Dip}TerP = GaCp* (**1a**) and ^{Tip}TerP = GaCp* (**1b**) accompanied by release of PMe_3. When warming the reaction mixture to ambient temperatures without irradiation, the clean re-formation of ^{Ar}TerP(PMe_3) and Cp*Ga in a second-order reaction was observed. Upon removal of PMe_3, **1a** and **1b** were isolated and fully characterized. Both derivatives were found to be labile and decomposed to the phosphafluorenes **2a** and **2b**, indicating generation of the transient phosphinidene ^{Ar}TerP along with Cp*Ga. First reactivity studies show that CO_2 and H_2O cleanly reacted with **1a**, affording ^{Dip}TerPCO (**3**) and ^{Dip}TerPH_2 (**4**), respectively.

Introduction

Heavier main group element–element multiple bond systems are no longer lab curiosities and tremendous effort has been devoted to establish new bonding patterns and to utilize the transition-metal like reactivity of these systems in terms of small molecule activation and functionalization.[1–11] Our group is interested in E^{13}–E^{15} multiple bond systems,[12] which are the iso-valent electronic heavier analogs of C–C multiple bond systems and have been proposed as intermediates in Metal–Organic Chemical Vapour Deposition (MOCVD) processes, which are based on utilizing molecular single-source E^{13}–E^{15} precursors.[13,14] The synthesis of E^{13}–E^{15} multiple bonds is challenging due to adjacent Lewis acidic E^{13} and Lewis basic E^{15} atoms, resulting in a tendency to oligomerize.[15–17] Just recently, our group isolated phospha- and arsaalumenes ^{Dip}TerPn = AlCp* and ^{Tip}TerP = AlCp* (^{Dip}Ter = 2,6-(2,6-i$Pr_2C_6H_3$)$_2$–C_6H_3; ^{Tip}Ter = 2,4,6-(2,46-i$Pr_3C_6H_3$)$_2$–C_6H_3; Cp* = C_5Me_5; Pn = P (**C**), As; Fig. 1)[18,19] by combining the pnictinidene transfer reagents ^{Ar}TerPn(PMe_3)[20] (Ar = Dip, Tip) with $(Cp^*Al)_4$ at 80 °C.[21,22] The heavier analogs of phosphaalumenes, phosphagallenes, have also been realized synthetically just recently, utilizing phosphanyl- or gallaphosphaketenes in the reaction with (^{Dip}Nacnac)Ga (^{Dip}Nacnac = HC[C(Me)NDip]$_2$) facilitating CO cleavage and formation of [(S)P]–P=Ga(^{Dip}Nacnac) (**A**; [(S)P] = (H_n-CNDip)$_2$P; $n = 1, 2$)[23] or (^{Dip}Nacnac)Ga=P–Ga(Cl)(^{Dip}Nacnac) (**B**, Fig. 1),[24] respectively. Reactivity studies revealed that **B** reacted directly at the Ga=P-bond and for example the reversible insertion of two CO_2 molecules, [2 + 2] cycloadditions with isocyanates and carbodiimides,[25] and 1,2-oxidative additions of E–H bonds were reported.[26] Interestingly, the phosphanyl-phosphagallene **A** showed mainly dipolar frustrated Lewis-pair (FLP) type 1,3-reactivity towards E–H bonds,[27] and with CO_2 the formation of a five-membered ring species with a P_2GaCO core was described.[23] We reasoned that the combination of Cp*Ga,[28,29] with ^{Ar}TerP(PMe_3) (Ar = Dip, Tip) would afford the

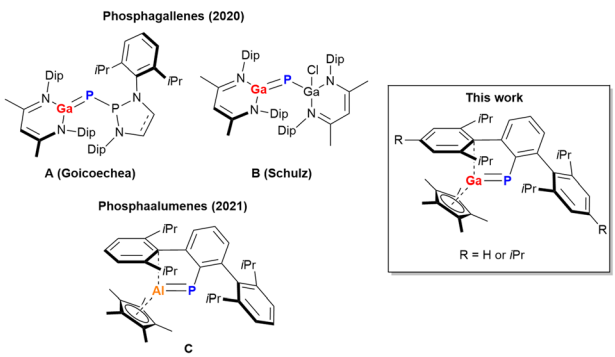

Fig. 1 Known phosphagallenes[23,24] and -alumenes[18] and the target of this study.

[a]*Leibniz Institut für Katalyse e.V. (LIKAT), A.-Einstein.-Str. 29a, 18059 Rostock, Germany. E-mail: jola.pospech@catalysis.de; christian.hering-junghans@catalysis.de; Web: https://www.catalysis.de/forschung/katalytische-funktionalisierungen; https://www.catalysis.de/forschung/katalyse-mit-erneuerbaren-rohstoffen/bioinspirierte-katalyse*

[b]*Institute of Chemistry, University of Rostock, A.-Einstein.-Str. 3a, 18059 Rostock, Germany. E-mail: jonas.bresien@uni-rostock.de; Web: https://www.chemie.uni-rostock.de/arbeitsgruppen/anorganische-chemie/dr-jonas-bresien/*

† Electronic supplementary information (ESI) available: Synthesis and characterization of compounds, NMR spectra, crystallographic, and computational details. CCDC 2216822–2216824. For ESI and crystallographic data in CIF or other electronic format see DOI: https://doi.org/10.1039/d2sc06292e

phosphagallenes ^{Ar}TerP = GaCp* by analogy with our strategy to access phospha- and arsaalumenes. Here we show that this transformation can be achieved photochemically and that in the presence of PMe_3 the reaction is fully reversible, indicating a facile and unusual ligand exchange at a phosphinidene center (Scheme 1).

Results and discussion

Synthesis and kinetic studies

Our investigations started with combining Cp*Ga and ^{Dip}TerP(PMe_3) in toluene-d_8, giving no discernible reaction at room temperature or when heated to 100 °C over a period of 72 h according to ^{1}H and ^{31}P NMR spectroscopy. Theoretical studies at the B3LYP-D3/def2-TZVP level of theory (*cf.* p. S34, ESI†) revealed an endergonic Cp*Ga for PMe_3 substitution ($\Delta_R G^\circ_{298} = +36.2$ kJ mol^{-1}) to give ^{Dip}TerP = GaCp* (**1a**). Irradiation of the NMR sample with an LED at 396 nm, which matches the longest wave-length absorption of ^{Dip}TerP(PMe_3) ($\lambda_{max,exp} = 381$ nm, $\lambda_{max,calcd} = 410$ nm), gave a color change from yellow to green within minutes (Scheme 1). Excitation of Cp*Ga can be excluded as it shows an absorption only in the UV-region ($\lambda_{max,exp} = 246$ nm, $\lambda_{max,calcd} = 241$ nm *cf.* Table S3†). In the absence of light, the green color faded and only ^{Dip}TerP(PMe_3) and Cp*Ga were detected by NMR spectroscopy, indicating the formation of the desired phosphagallene **1a** in reversible fashion. Recently, the reversible phosphinidene transfer in a stannaphosphene has been reported.[30] We next irradiated a toluene-d_8 solution containing ^{Dip}TerP(PMe_3) and Cp*Ga in a 1 : 1 ratio inside the NMR spectrometer using a laser diode ($\lambda = 405$ nm, 140 mW).

The formation of **1a** was traced by ^{1}H and ^{31}P NMR spectroscopy at room temperature, showing two new resonances in the ^{31}P NMR spectrum at −62.9 ppm (PMe_3) and −104.8 ppm for **1a**, which corresponds well with the theoretically predicted value for **1a** ($\delta(^{31}P)_{calcd} = -105.2$ ppm). After irradiation for 2 h a dynamic steady state between **1a**, PMe_3 and ^{Dip}TerP(PMe_3), Cp*Ga was reached. When switching off the laser the concentration of **1a** and PMe_3 decreased, and the starting materials were re-formed. Irradiation at −20 °C gave **1a** nearly quantitatively, effectively suppressing the thermal back reaction. The thermal reverse reaction was then studied at 10, 15, 20 and 25 °C using the same sample repeatedly, indicating a fully reversible system. Using the concentrations derived from the relative integrals of **1a**, PMe_3, Cp*Ga and ^{Dip}TerP(PMe_3) in the ^{1}H NMR data, the reaction kinetics of the thermal reverse reaction were investigated. The reaction follows 2nd order kinetics. However, the concentration profiles could be described reasonably well using two different models, one including an associative (nucleophilic attack of PMe_3 at **1a** in a S_N2-type reaction), the other a dissociative mechanism (with the dissociation reaction **1a** ⇌ ^{Dip}TerP + Cp*Ga as its first step and reaction with PMe_3 in a subsequent step; *cf.* p. S30†).Thus, the experimental data alone do not allow a definitive statement regarding the mechanism of the reaction. Yet, since the dissociative mechanism would include free phosphinidenes, albeit in very low concentrations, it is certainly less likely. Nonetheless, both models gave similar activation barriers ($\Delta G^\ddagger \approx 90$ kJ mol^{-1}, Table S6†) when analyzing the temperature dependence of the rate constants using transition state theory (TST).

To investigate the possible mechanism of the thermal reverse reaction further, we performed a series of semi-empirical GFN2-*x*TB computations[31] as well as DFT calculations at the B3LYP-D3/def2-TZVP level of theory (*cf.* p. S46†).[32–34] We could in fact identify both an associative as well as a dissociative reaction pathway. The associative S_N2-type mechanism involves an activation barrier of $\Delta G^\ddagger = 80.1$ kJ mol^{-1} ($\Delta G^\ddagger_{exptl.} = 87 \pm 12$ kJ mol^{-1}, TS2, Scheme 2), in good agreement with the experimental data. A second potential associative pathway, involving a weak donor–acceptor complex between PMe_3 and **1a** was also identified, however this path is associated with a significantly higher barrier ($\Delta G^\ddagger = 121.4$ kJ mol^{-1}, TS1, Scheme 2) and is therefore not in line with the experimental values. The free dissociation energy of **1a** into PMe_3 and singlet ^{Dip}TerP, on the other hand, was estimated at +107.2 kJ mol^{-1} (note a rather high uncertainty for this value due to the singlet biradical character of ^{Dip}TerP, which is not well represented within DFT), which puts this first reaction step of the dissociative pathway in a reasonable energetic range. Assuming a low activation barrier for this dissociative pathway, it lies in

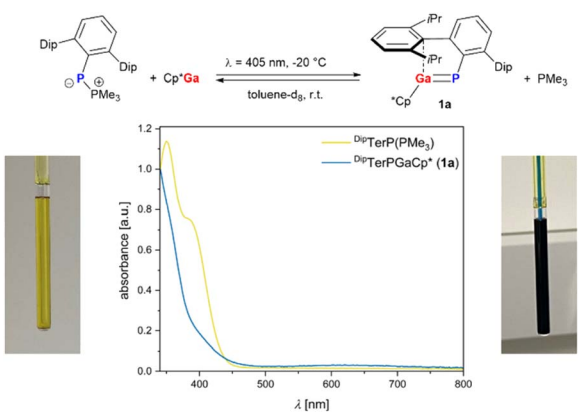

Scheme 1 Reversible formation of ^{Dip}TerPGaCp* (**1a**). Images of the reaction solution before (bottom left) and after irradiation (bottom right) along with the UV absorption spectra of ^{Dip}TerP(PMe_3) and **1a** (in *n*-hexane, bottom middle).

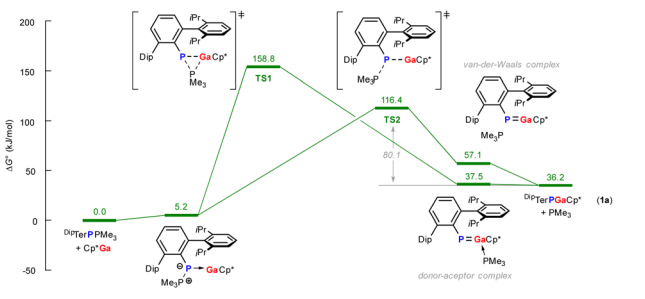

Scheme 2 Computed reaction pathway for the thermal reverse reaction of **1a** with PMe_3 (B3LYP-D3/def2-TZVP, $c^\circ = 1$ mol L^{-1}).

a similar energy window as the S_N2-type substitution with PMe_3, and thus could be a (minor) contributing factor to the thermal reverse reaction. Note that singlet ^{Dip}TerP would only be formed *in situ*, as it is predicted to possess a triplet ground state (ΔE_{S-T} = 45.5 kJ mol^{-1}). Singlet phosphinidenes have previously been shown to be electrophilic and irreversible ligand exchange reactions were described.[35–37]

Characterization

Next, we sought to isolate **1a** rather than generating it *in situ*.

A flask containing a 1 : 1 mixture of ^{Dip}TerP(PMe_3) and Cp*Ga in toluene was connected to a receiving flask *via* a U-shaped glass tube and the headspace was evacuated (Scheme 3, top). After irradiating the mixture for 4 h (λ_{LED} = 396 nm) a color change to deep green was observed and the receiving flask was then cooled to *ca.* −70 °C to slowly evaporate PMe_3 and toluene into the receiving flask, while the product crystallized in the reaction flask. After washing with *n*-heptane at −78 °C, **1a** was isolated as a dark turquoise solid in good yield (77%). X-ray quality crystals of **1a** were grown from a saturated *n*-hexane solution at −30 °C.

The ^{1}H NMR data of **1a** are similar to those of ^{Dip}TerPAlCp* (**C**) with three characteristic signals for the Dip-groups in the alkyl region and a singlet resonance for the Cp*-substituent, indicating η^5-coordination, or at least a fast sigmatropic rearrangement in solution. The ^{31}P NMR signal of **1a** ($\delta(^{31}P)(C_6D_6)$ = −104.8 ppm; $\delta(^{31}P)(C_7D_8)$ = −105.5 ppm) is significantly deshielded compared to **C** (*cf.* $\delta(^{31}P)$ = −203.9 ppm). The Ga–P stretching vibration in **1a** at 448 cm^{-1} (calcd 439 cm^{-1}) is red-shifted compared to the Al–P stretch in **C** at 558 cm^{-1} in the IR spectrum, while the lowest energy absorption in the UV-vis ($\lambda_{max,exp}$ = 620 nm, $\lambda_{max,calcd}$ = 635 nm) is similar to that in ^{Dip}TerAsAlCp* (λ_{max} = 590 nm).[5]

1a crystallizes in the monoclinic space group $P2_1/c$ and is isomorphous with **C** with a P–Ga distance of 2.2104(5) Å (*cf.* **C** 2.2113(6); $\sum r_{cov}$(P=Ga) = 2.19 Å)[38] and a C1–P1–Ga1 angle of 105.02(5)°(Fig. 2, left), minimally narrower than in **C**, resulting in a close contact between Ga1 and one of the flanking Dip-groups of the ^{Dip}Ter-moiety (d(Ga1–C19) = 2.8869(15) Å).[17]

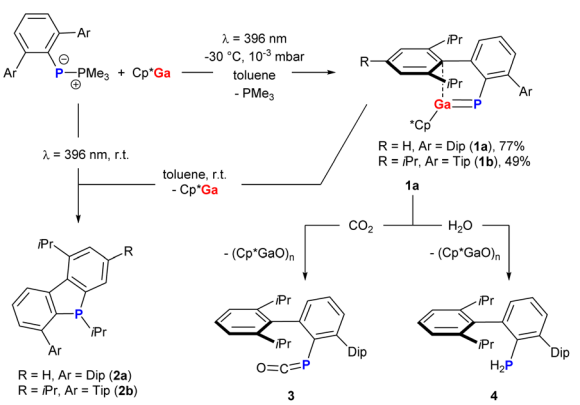

Scheme 3 Isolation of **1a** and **1b**, its thermal decomposition and reactivity of **1a** towards CO_2 and H_2O.

The Ga–C_{Cp*} distances range from 2.1526(18) to 2.5202(17), with two short and three rather long contacts, indicating that in the solid state the Cp* substituent is not perfectly η^5-coordinated.

Starting from ^{Tip}TerP(PMe_3), ^{Tip}TerPGaCp* (**1b**, 49%), was synthesized in similar fashion and X-ray quality crystals of **1b** were grown from a saturated *n*-heptane solution at −30 °C, revealing similar structural parameters compared to **1a** (Fig. 2, middle), with a short Ga1–P1 atomic distance of 2.2176(5) Å and a similar short Ga1···C_{Tip} contact (d(Ga1–C7) = 2.8555(16) Å) and a C1–P1–Ga1 angle of 104.44(6)°. This shows that the terphenyl moiety has minimal influence on the structure of **1**. **1b** showed a singlet signal in the ^{31}P NMR spectrum at −109.8 ppm in C_6D_6 (calcd −107.9 ppm) and in the ^{1}H NMR spectrum two characteristic resonances in a 2 : 1 ratio were detected for the methine protons of the ^{Tip}Ter-substituent, along with three doublet signals for the iPr-groups and one singlet for the Cp* substituent at Ga.

Surprisingly, even isolated **1a** and **1b** are thermally labile in solution. Particularly for **1b** decomposition was already observed after 10 min in C_6D_6 solution, with new signals at 1.91 and at 0.9 ppm in the ^{1}H NMR spectrum indicating the formation of Cp*Ga and a phosphafluorene (**2b**, Scheme 3), previously observed when ^{Tip}TerP(PMe_3) was irradiated at λ = 365 nm.[39] Albeit slower, **1a** showed a similar behavior in solution, decomposing to give Cp*Ga and the related phosphafluorene **2a**. The thermal decomposition in C_7D_8 solution was then studied by ^{1}H NMR spectroscopy over time, which revealed a 1st order decay of **1a** and **1b** with half lives of 47.8 and 7.8 h, respectively. This compares well with the theoretically determined free dissociation energy of **1a** into ^{Dip}TerP and Cp*Ga ($\Delta G_{diss,calcd}$ = 107.2 kJ mol^{-1}, $\Delta G^{\ddagger}_{exptl.} \approx 104 \pm 5$ kJ mol^{-1}; *cf.* Section in the ESI†) and corroborates the formation of **2a** as decomposition product of ^{Dip}TerP. Moreover, the faster decomposition of **1b** can be understood in terms of electrophilic attack of the phosphinidene on one of the flanking aryl groups, which should be faster for the more electron-rich Tip-substituent present in **1b**.

Electronic structure

The electronic structure of **1a** was probed using NBO,[40,41] AIM,[42,43] and ELF analyses.[44] The P–Ga bonding is best described as a polarized double bond (Scheme 4): The σ bond, which is formed by the 3p$_x$(P) and 4s(Ga) orbitals, is evenly distributed between both atoms. The π bond, on the other hand, is strongly polarized towards the P atom [~87% 3p$_z$(P), ~13% 4p$_z$(Ga); resonances type **II** and **III**], which agrees with the NBO data for known variants **A** and **B**.[23,24] The polarization of the P–Ga double bond is also reflected in the natural charges of P (−0.28*e*) and Ga (+1.11*e*) as well as in the Wiberg bond index of 1.31. In structure **II-a**, there are two formal lone valences at the Ga atom (4p$_x$ and 4p$_y$ orbitals), which are stabilized by donor–acceptor interactions with the s-type LP at the P atom (resonance **I**) as well as the Cp* ligand (resonances of type **b**), respectively (see also Scheme S2†). Note that resonance **I**, to which we attribute only a small weight, should be understood in

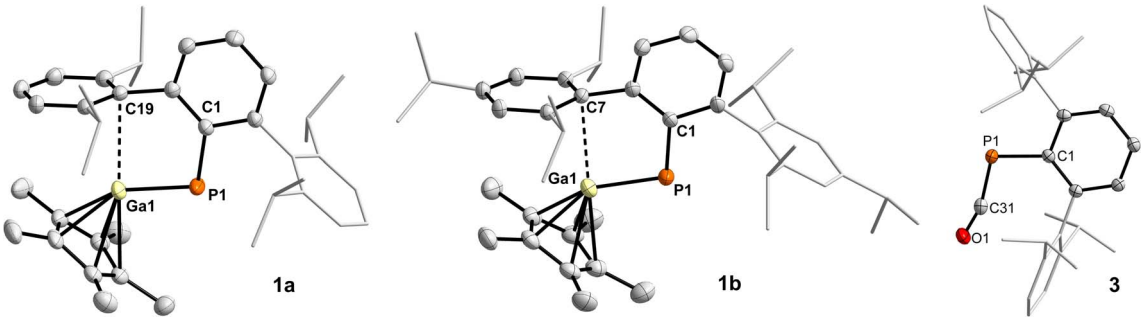

Fig. 2 Molecular structures of **1a** (left), **1b** (middle) and **3** (right). ORTEPs drawn at 50% probability. Selected bond lengths (Å) and angles (°) of **1a**: P1–Ga1 2.2104(5), Ga1–C19 2.8869(15); C1–P1–Ga1 105.02(5); **1b**: P1–Ga1 2.2176(5), Ga1–C7 2.8555(16); C1–P1–Ga1 104.44(6); **3**: P1–C31 1.6833(12), C311–O1 1.1559(14); C1–P1–C311 105.17(5), P1–C31–O1 162.45(10).

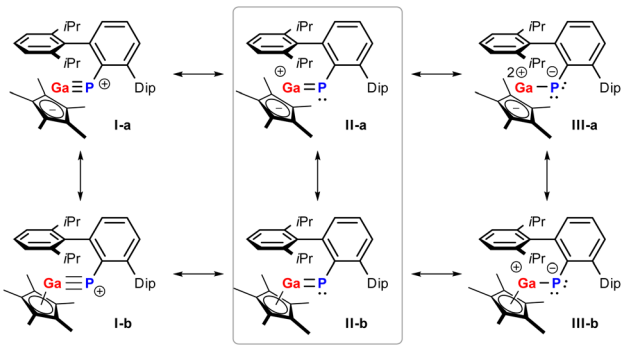

Scheme 4 Lewis resonance scheme of compound **1a**.

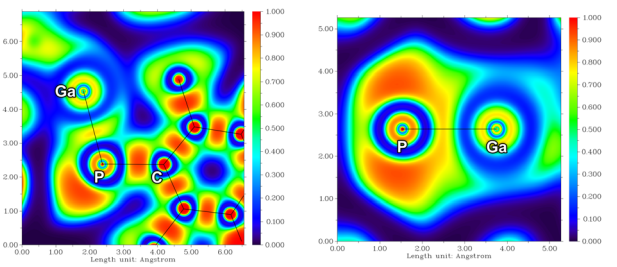

Fig. 3 ELF of **1a** in the Ga–P–C plane (left) and perpendicular to that plane (right).

terms of a non-classical multiple bond, *i.e.* the LP(P) → 4p$_x$(Ga) interaction is not a π bond (in-depth description of the electronic structure, p. S40ff†). Inspection of the Electron Localization Function (ELF, Fig. 3) supported the results from NBO analysis, with a LP on the P atom and strongly polarized π-electron density towards the P atom perpendicular to the Ga–P–C$_{Ter}$ plane, in line with resonance between Lewis structures **II** and **III** (Scheme 3).

Inspection of the Laplacian of the electron density $\nabla^2\rho$ corroborates charge accumulation near the P atom in the π bonding system, in agreement with the NBO and ELF results. The ellipticity ε at the bond critical point (BCP) of 0.31 indicates double bond character (*cf.* ∼0.3 for ethylene, ∼0.2 for benzene; Table S15†).

Reactivity studies

Next, we tested the reactivity of **1a** towards CO_2. Phosphagellenes were previously shown to react with CO_2 to give five-membered ring species[23] or to reversibly insert two CO_2 molecules into the Ga–P bond.[24] When a green toluene-d_8 solution of **1a** was exposed to an atmosphere of CO_2 a color change to orange was observed after 20 min at room temperature.

A resonance in the $^{31}P\{^1H\}$ NMR spectrum at −201.3 ppm, along with a doublet in the ^{13}C NMR spectrum at 199.9 ppm ($^1J_{PC} = 102.4$) indicated the formation of the arylphosphaketene ^{Dip}TerPCO (**3**), which was verified by SC-XRD experiments on crystals grown from *n*-hexane at −30 °C. Additionally, a broad feature between 1.65–2.01 ppm in the ^1H NMR spectrum with an integral value of *ca.* 15 indicated the formation of various Cp*-containing species. The PCO unit in **3** is in-plane with the central aryl ring of the ^{Dip}Ter-substituent, and deviates from linearity (∢(P1–C31–CO) = 162.45(10)°) with short P1–C31 (1.6833(12) Å) and C31–O1 (1.1559(14) Å) distances (Fig. 2, right). Surprisingly, **3** represents the first structurally characterized arylphosphaketene. Phosphaketene, *t*Bu–PCO, was first isolated by Appel and Paulen in 1983 through treatment of *t*BuP(SiMe$_3$)$_2$ with phosgene at −70 °C, with a characteristic ^{31}P NMR shift of −180 ppm. In the same year Mes*PCO (Mes* = 2,4,6-*t*Bu$_3$C$_6$H$_2$) was isolated as stable orange crystalline solid,[45] and has been utilized as phosphinidene transfer reagent.[46,47] Recently, the chemistry of phosphaketenes has seen a resurgance based on Na(dioxane)$_x$PCO as an easily accessible form of the phosphaethynolate anion [PCO]$^-$,[48] allowing to access heteroatom-substituted E–PCO systems through salt metathesis reactions.[23,24,35–37,49–51] The deoxygenation of CO_2 to access **3** is reminiscent of the bora-phospha-Wittig reaction, in which phosphaborenes are utilized to make phosphaalkenes.[52] Due to the presence of Cp*-containing impurities it was not possible to isolate **3** in pure form, however, it can be generated *in situ* in clean fashion, which will allow further reactivity studies in the future.

With H_2O **1a** reacted to give ^{Dip}TerPH$_2$ (**4**) quantitatively,[53] clearly underlining the potential of **1a** to act as an deoxygenation reagent, while also clearly deviating from the reactivity of ^{Dip}TerP(PMe$_3$) towards H_2O, which afforded the primary phosphine oxide ^{Dip}TerP(O)H$_2$ instead.[54]

Conclusion

Phosphagallenes have previously been obtained by reacting phosphaketenes with the Ga(I) source ^{Dip}NacnacGa as thermally stable entities. Here we show that ^{Dip}TerPGaCp* (**1a**) is only formed upon irradiation of ^{Dip}TerP(PMe_3) in the presence of Cp*Ga. Under thermal conditions **1a** reacted with PMe_3 back to the starting materials in a 2nd-order reaction, indicating a facile and reversible PMe_3 for Cp*Ga exchange at a phosphinidene. When removing PMe_3 while irradiating the reaction mixture, **1a** and **1b** were isolated. However, in solution the isolated phosphagallenes dissociate into the phosphinidene ^{Ar}TerP and Cp*Ga. ^{Ar}TerP is highly reactive and formed the phosphafluorenes **2a** and **2b**. The bonding in **1a** was investigated by combined theoretical means (NBO, ELF, AIM), clearly showing a strongly polarized (towards P) P–Ga bond with significant double bond character. Considering the longer half-life of **1a**, its reactivity towards CO_2 and H_2O was probed, giving phosphaketene **3** and phosphine **4**, respectively. Further reactivity studies to harness the reversible formation of **1a** and its lability with respect to phosphinidene release are currently underway.

Data availability

Crystallographic data for **1a**, **1b** and **3** has been deposited at the CCDC under 2216822–2216824. The datasets supporting this article have been uploaded as part of the ESI.†

Author contributions

J. P., J. B. and C. H.-J. conceptualized the project and designed the experiments. T. T., J. B. and C. H.-J. carried out most of the experimental work. T. T., F. D., J. B., J. P. and C. H.-J. characterized the compounds and analyzed the data. D. M., J. B. and C. H.-J. performed the *in situ* NMR studies and analyzed the data. J. B. carried out the computational studies. The manuscript was written through contributions of all authors. All authors have given approval to the final version of the manuscript.

Conflicts of interest

There are no conflicts to declare.

Acknowledgements

F. D. and C. H.-J. thank the Leibniz Association for funding within the scope of the Leibniz ScienceCampus Phosphorus Research Rostock (**https://www.sciencecampus-rostock.de**). We wish to thank the ITMZ at the University of Rostock for access to the cluster computer, and especially Malte Willert for his assistance with the queuing system and software installations.

Notes and references

1 L. Weber, *Chem. Rev.*, 1992, **92**, 1839–1906.
2 P. P. Power, *Chem. Rev.*, 1999, **99**, 3463–3504.
3 Y. Wang and G. H. Robinson, *Chem. Commun.*, 2009, 5201–5213.
4 R. C. Fischer and P. P. Power, *Chem. Rev.*, 2010, **110**, 3877–3923.
5 P. P. Power, *Acc. Chem. Res.*, 2011, **44**, 627–637.
6 P. Bag, C. Weetman and S. Inoue, *Angew. Chem., Int. Ed.*, 2018, **57**, 14394–14413.
7 T. Chu and G. I. Nikonov, *Chem. Rev.*, 2018, **118**, 3608–3680.
8 J.-D. Guo and T. Sasamori, *Chem.–Asian J.*, 2018, **13**, 3800–3817.
9 C. Weetman and S. Inoue, *ChemCatChem*, 2018, **10**, 4213–4228.
10 R. L. Melen, *Science*, 2019, **363**, 479–484.
11 R. Borthakur and V. Chandrasekhar, *Coord. Chem. Rev.*, 2021, **429**, 213647.
12 F. Dankert and C. Hering-Junghans, *Chem. Commun.*, 2022, **58**, 1242–1262.
13 S. Schulz, in *Advances in Organometallic Chemistry*, Academic Press, 2003, vol. 49, pp. 225–317.
14 M. A. Malik, M. Afzaal and P. O'Brien, *Chem. Rev.*, 2010, **110**, 4417–4446.
15 M. Kapitein and C. von Hänisch, *Eur. J. Inorg. Chem.*, 2015, **2015**, 837–844.
16 M. Kapitein, M. Balmer, L. Niemeier and C. von Hänisch, *Dalton Trans.*, 2016, **45**, 6275–6281.
17 S. Nees, F. Fantuzzi, T. Wellnitz, M. Fischer, J.-E. Siewert, J. T. Goettel, A. Hofmann, M. Härterich, H. Braunschweig and C. Hering-Junghans, *Angew. Chem., Int. Ed.*, 2021, **60**, 24318–24325.
18 M. Fischer, S. Nees, T. Kupfer, J. T. Goettel, H. Braunschweig and C. Hering-Junghans, *J. Am. Chem. Soc.*, 2021, **143**, 4106–4111.
19 S. Nees, T. Wellnitz, F. Dankert, M. Härterich, S. Dotzauer, M. Feldt, H. Braunschweig and C. Hering-Junghans, *Angew. Chem., Int. Ed.*, 2023, e202215838.
20 P. Gupta, J.-E. Siewert, T. Wellnitz, M. Fischer, W. Baumann, T. Beweries and C. Hering-Junghans, *Dalton Trans.*, 2021, **50**, 1838–1844.
21 C. Dohmeier, C. Robl, M. Tacke and H. Schnöckel, *Angew. Chem., Int. Ed.*, 1991, **30**, 564–565.
22 H. Sitzmann, M. F. Lappert, C. Dohmeier, C. Üffing and H. Schnöckel, *J. Organomet. Chem.*, 1998, **561**, 203–208.
23 D. W. N. Wilson, J. Feld and J. M. Goicoechea, *Angew. Chem., Int. Ed.*, 2020, **59**, 20914–20918.
24 M. K. Sharma, C. Wölper, G. Haberhauer and S. Schulz, *Angew. Chem., Int. Ed.*, 2021, **60**, 6784–6790.
25 M. K. Sharma, C. Wölper, G. Haberhauer and S. Schulz, *Angew. Chem., Int. Ed.*, 2021, **60**, 21784–21788.
26 M. K. Sharma, C. Wölper and S. Schulz, *Dalton Trans.*, 2022, **51**, 1612–1616.
27 J. Feld, D. W. N. Wilson and J. M. Goicoechea, *Angew. Chem., Int. Ed.*, 2021, **60**, 22057–22061.
28 D. Loos and H. Schnöckel, *J. Organomet. Chem.*, 1993, **463**, 37–40.
29 P. Jutzi and L. O. Schebaum, *J. Organomet. Chem.*, 2002, **654**, 176–179.

30 M. Fischer, M. M. D. Roy, L. L. Wales, M. A. Ellwanger, A. Heilmann and S. Aldridge, *J. Am. Chem. Soc.*, 2022, **144**, 8908–8913.
31 C. Bannwarth, E. Caldeweyher, S. Ehlert, A. Hansen, P. Pracht, J. Seibert, S. Spicher and S. Grimme, *Wiley Interdiscip. Rev.: Comput. Mol. Sci.*, 2021, **11**, e1493.
32 H. Jonsson, G. Mills and K. W. Jacobsen, in *Classical and Quantum Dynamics in Condensed Phase Simulations*, 1998, pp. 385–404.
33 F. Neese, F. Wennmohs, U. Becker and C. Riplinger, *J. Chem. Phys.*, 2020, **152**, 224108.
34 F. Neese, *Wiley Interdiscip. Rev.: Comput. Mol. Sci.*, 2022, **12**, e1606.
35 M. M. Hansmann and G. Bertrand, *J. Am. Chem. Soc.*, 2016, **138**, 15885–15888.
36 M. M. Hansmann, R. Jazzar and G. Bertrand, *J. Am. Chem. Soc.*, 2016, **138**, 8356–8359.
37 L. Liu, D. A. Ruiz, D. Munz and G. Bertrand, *Chem*, 2016, **1**, 147–153.
38 P. Pyykkö and M. Atsumi, *Chem.–Eur. J.*, 2009, **15**, 12770–12779.
39 S. Shah, M. C. Simpson, R. C. Smith and J. D. Protasiewicz, *J. Am. Chem. Soc.*, 2001, **123**, 6925–6926.
40 E. D. Glendening, A. E. Reed, J. E. Carpenter, J. A. Bohmann, C. M. Morales, C. R. Landis and F. Weinhold, *Theoretical Chemistry Institute*, University of Wisconsin, Madison, WI, 2013.
41 F. Weinhold, C. R. Landis and E. D. Glendening, *Int. Rev. Phys. Chem.*, 2016, **35**, 399–440.
42 R. F. W. Bader, *Atoms in Molecules: A Quantum Theory*,Oxford University Press, 1994.
43 T. Lu and F. Chen, *J. Comput. Chem.*, 2012, **33**, 580–592.
44 A. D. Becke and K. E. Edgecombe, *J. Chem. Phys.*, 1990, **92**, 5397–5403.
45 R. Appel and W. Paulen, *Angew. Chem., Int. Ed. Engl.*, 1983, **22**, 785–786.
46 A. H. Cowley, B. Pellerin, J. L. Atwood and S. G. Bott, *J. Am. Chem. Soc.*, 1990, **112**, 6734–6735.
47 A. H. Cowley, F. Gabbai, R. Schluter and D. Atwood, *J. Am. Chem. Soc.*, 1992, **114**, 3142–3144.
48 J. M. Goicoechea and H. Grützmacher, *Angew. Chem., Int. Ed.*, 2018, **57**, 16968–16994.
49 A. R. Jupp and J. M. Goicoechea, *J. Am. Chem. Soc.*, 2013, **135**, 19131–19134.
50 D. Heift, Z. Benkő and H. Grützmacher, *Dalton Trans.*, 2014, **43**, 5920–5928.
51 K. M. Szkop, A. R. Jupp, H. Razumkov and D. W. Stephan, *Dalton Trans.*, 2020, **49**, 885–890.
52 A. M. Borys, E. F. Rice, G. S. Nichol and M. J. Cowley, *J. Am. Chem. Soc.*, 2021, **143**, 14065–14070.
53 W. A. Merrill, E. Rivard, J. S. DeRopp, X. Wang, B. D. Ellis, J. C. Fettinger, B. Wrackmeyer and P. P. Power, *Inorg. Chem.*, 2010, **49**, 8481–8486.
54 F. Dankert, M. Fischer and C. Hering-Junghans, *Dalton Trans.*, 2022, **51**, 11267–11276.